Effect of Multi-Walled Carbon Nanotubes Addition on Mechanical Properties of Polymer Composites Laminate

Ming-Chuen Yip[1], Yi-Chieh Lin[1], and Chung-Lin Wu[2,*]

[1]Department of Power Mechanical Engineering, National Tsing Hua University, Hsinchu 30013 Taiwan, ROC

[2]Center for Measurement Standards, Industrial Technology Research Institute, Hsinchu 30011 Taiwan, ROC

SUMMARY

Carbon nanotubes (CNTs) have high potential for the modification of glass-fiber reinforced polymer (GFRP) composite laminates. This paper reports the fabrication of CNTs/GFRP composite laminates using ultrasonication and the hand lay-up method. The aim of this study is to investigate the interlaminar shear strength (ILSS) and flexural strength of composites consisting of several different proportions of CNTs. When CNT content is 0.75 percent hundred resin (phr), the mechanical properties are the best. The ILSS was significantly improved 15.7% and flexural strength improved 9.2%. The effects of addition of CNTs on the mechanical performances were evaluated with respect to retention of high-temperature properties up to 200 °C. It was found that ILSS, flexural strength and bending modulus were significantly enhanced by CNTs at different temperatures. Dynamic mechanical analysis (DMA) was employed to measure the storage modulus of composite laminates. To consider the effect of temperature on GFRP and CNTs/GFRP composite laminates, the results showed the trends in the temperature-dependence and were nearly identical to the ILSS, flexural strength, bending modulus and dynamic properties. The experimental fracture surfaces were also observed by scanning electron microscopy (SEM). Significant weakening of fiber-matrix interface and matrix softening were major factors affecting the strength and modulus reduction at high temperature.

1. INTRODUCTION

Advanced GFRP composites have long been used as viable primary load-bearing structures. Compared to metals, the GFRP composite laminates have many advantages such as higher fatigue strength, higher corrosion resistance and lower weight[1]. However, GFRP composite laminates are subject to effects of flexure, compression and tension, which can lead to interlayer delamination because the thickness properties are often insufficient, due to the weak glass fiber-matrix interface[2].

As is well known, carbon nanotubes were found in an electrical arc discharge[3]. The nanocomposites filled with CNTs have been shown to possess superior mechanical, electrical and thermal properties[4-7]. In order to achieve optimal enhancement in the property of the CNTs/GFRP composite laminates key issues to consider are: (i) an appropriate dispersion of the reinforcement in the matrix, (ii) the alignment of CNT, (iii) the different types of nanofillers and (iv) the interfacial strength[8-11]. When compared to the neat resin matrix, the Young's modulus and the yield strength were doubled and quadrupled for nanocomposites with 1.0 and 4.0 wt.% nanotubes, respectively[12]. Tai *et al.*[13] presented a double increment in tensile strength of the MWNTs/phenolic nanocomposites when 3.0 wt.% CNT was introduced into the phenolic matrix. The fabrication of CNT reinforced composite is the homogeneous dispersion of the MWNT in the polymer matrix so that it has uniform properties and can efficiently handle load transfer during structural excitation[14–16]. Among those studies, little attention was paid to the effect of temperature on the ILSS, flexural strength and bending modulus of the GFRP and CNTs/GFRP composite laminates described above.

Therefore, the ILSS, flexural strength, bending modulus and storage modulus for GFRP and CNTs/GFRP composite laminates are calculated in this paper. The strength and modulus of those composite laminates at temperatures up to 200 °C were also investigated.

2. SPECIMENS MANUFACTURE AND EXPERIMENTS

2.1 Materials

In this study multi-walled carbon nanotubes (MWCNTs) were supplied by DESUN Nano Company. The CNTs synthesized by the chemical vapor deposition (CVD) process had an average diameter of 30-50 nm and a length of 10-200 μm. An epoxy resin was selected as the polymer

*Corresponding author e-mail: clwu@itri.org.tw

matrix because it is known that CNTs are dispersed well in the epoxy resin compared with other polymer resins. The epoxy resin was developed by Wah Hong Industrial Corporation called the WH-EP001 (based on Bisphenol-A), which produces a hard, highly crosslinked thermoset with high solvent resistance and relatively high impact strength. The composite specimens for mechanical properties testing were constructed using bi-directional woven E-glass fiber reinforcement (supplied by Wah Hong Industrial Corporation). The fabric is fairly coarse with 44 tows/inch in the warp direction and 32 tows/inch in the woof direction (**Figure 1**). There are approximately 400 glass filaments (fibers) in each bundle (tow).

2.2 Manufacturing

2.2.1 Preparation of Nanotube-Prepregnated Woven Glass Fiber

The CNTs prepared were composed of many aggregates of different sizes. The aggregates would be obstacles to uniform dispersion of the CNTs, and were hardly broken into individual tubes in the epoxy resin. Epoxy composites containing well-dispersed CNTs were prepared by the following procedures. The 0.25, 0.5, 0.75, 1.0 phr CNTs and surfactant (Triton X-100) were first dispersed in acetone under ultra-sonication at a frequency of 40 kHz and magnetic stirring. The CNTs/acetone solutions with different CNT weight fractions were then mixed with the epoxy resin. The mixture was also sonicated for 1.5h at 60 °C. The plain weave glass fabric was manually impregnated with the mixture. The prepreg was kept in a vacuum oven for 1 hr at 75 °C to remove air bubbles and the acetone.

2.2.2 Fabrication of CNT Reinforced Polymer Composites

The composite laminate panels 200 mm × 180 mm were fabricated by hand layup with 6 plies. The layup was done in a Teflon peel ply and a bleeder was placed on the top of panel with more than 1000 psi of pressure. The bleeder was laid down in such a way as to remove the air bubbles from the epoxy. The laminates were cured at 140 °C for 0.5 hr. All specimens were then post-cured at 90 °C for 12 hours to improve the polymerization at the interface in the presence of CNTs. This procedure produced composite laminates with a thickness between 2.65 and 2.75 mm.

2.3 Experimental Methods

2.3.1 Interlaminar Shear Strength Tests

The interlaminar shear strength (ILSS) tests were carried out in accordance to ASTM D2344, using at least six specimens (short beam: 21 mm × 6.35 mm × 2.7 mm) for each laminate family. These tests were performed in a universal testing machine (Instron 8848 1KN) at constant cross-speed of 1.3 mm/min, at room temperature. The calculation was based on Equation (1).

$$\text{Interlaminar shear strength} = \frac{0.75P}{be} \quad (1)$$

where P is the failure load, b and e are specimen width and thickness, respectively.

2.3.2 Flexural tests

The flexural tests were carried out in accordance to ASTM D790 (3-point bending), using a minimum of five specimens (dimensions: 60mm × 40mm × 2.7mm) for each laminate family. These tests were performed in a universal testing machine (Instron 8848 1 KN) at a constant cross-speed of 1.3 mm/min, at room temperature, using an appropriate device for flexural test.

Equation (2) was used to calculate the flexural strength.

$$\text{Flexural strength} = \frac{3PL}{2be^2} \quad (2)$$

where P is the failure load, L, b and e are the support span, specimen width and specimen thickness, respectively.

2.3.3 Dynamic Mechanical Analysis

Dynamic mechanic analysis (DMA) was performed on a TA Q800 operating in the three-point bending mode at an oscillation frequency of 1 Hz. The storage modulus and loss modulus were measured from the room temperature to 200 °C at a scanning rate of 3 °C/min. Three specimens were cut by a diamond saw in the form of rectangular beams of a nominal 36 mm × 13 mm × 2.7 mm. The glass transition temperatures (T_g) of the composite laminates were determined by DMA from peaks in the tan delta curve.

Figure 1. Cross-section of the GFRP composite laminate tested in this report shows void-free quality composites

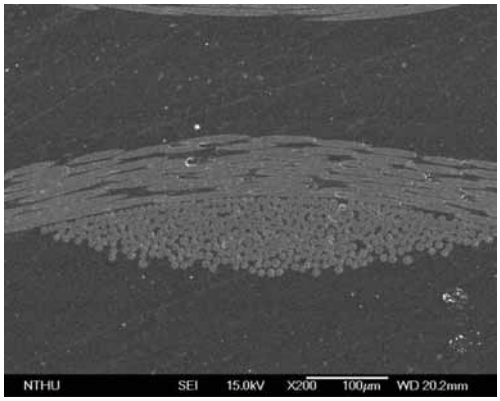

2.3.4 Strength of the Composite Laminates at High Temperature

The ILSS tests and flexural tests were performed at 25-200 °C. All tests were conducted in displacement control using an Instron 8848 micro tester. Specimens were heated by enclosure in a high temperature oven until the testing temperature was reached. Specimens were heat-soaked for at least 15 min prior to loading to ensure homogeneous temperature distribution. To perform tensile test specimens were preloaded to 0.5 N. A constant crosshead speed of 1.3 mm/min was used to bend specimens to failure. While multiple samples were tested at room temperature to determine the standard variation in the ILSS, flexural strength and bending modulus, only one or two specimens were tested at various temperatures between 50-200 °C.

2.3.5 Scanning Electrical Microscopy

The fiber-matrix adhesion and fracture behavior after mechanical testing were analyzed with field emission gun scanning electron microscopy (FEG-SEM). FEG-SEM images were obtained with JEOL JSM-6330F operating at 15 kV to examine the fracture; surfaces of specimens from shear failure ply were sputter-coated with a thin layer of gold for FEG-SEM observation.

Figure 2. Effect of CNT contents on ILSS of GFRP composite laminates

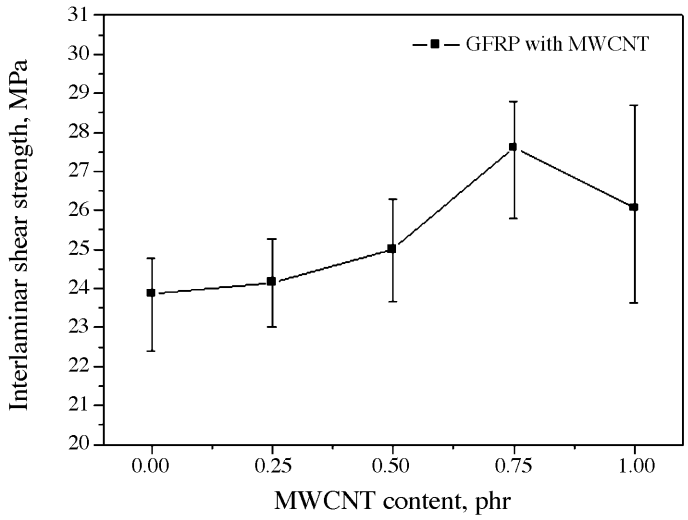

Figure 3. SEM micrograph of ILSS test, showing an agglomeration particle in 0.75 phr CNTs/GFRP composite laminates fracture surface

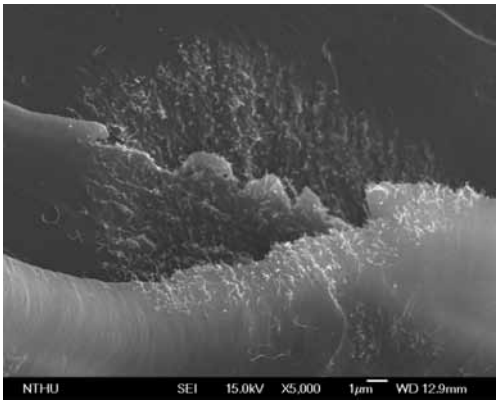

3. RESULTS AND DISCUSSION

3.1 Interlaminar Shear Strength Tests

All data, including statistical deviation, from the short beam shear tests of the CNTs/GFRP composite laminates with different CNTs content are shown in **Figure 2**. When the content of the CNTs is low, the strengthening effect is not remarkable. With the increase of the CNTs to 0.75 phr, the ILSS is the best. The ILSS can be increased from 23.8 to 27.6 MPa, a rise of 15.7%. By adding CNTs, the above-mentioned relative improvement of GFRP composite laminates in strength can be explained by the high specific mechanical property and specific surface area of the CNTs. Here, CNTs play the role of the enhancing materials. With further increase of the content of CNTs, it is easy to induce agglomeration of CNTs (**Figure 3**). The agglomeration influences the effect of CNTs surface area and reduces the ILSS. The property of ILSS is however still stronger than that of GFRP composite laminates.

The ILSS of GFRP composite laminates depends strongly on the fiber-matrix adhesion. Adding CNTs can improve the ability to transfer the stress between the matrix and fibers. SEM photomicrographs of GFRP fracture surfaces are shown in **Figure 4a**. During the short beam shear testing, the primary failure mode is a delamination along the glass-fiber/matrix interface; the figure shows the matrix completely detached from the fiber surface due to weak adhesion evidenced by smooth and clean fiber surface. In comparison, CNTs/GFRP composite laminate specimens can be distinguished by the development of a significantly different interface microstructure shown on the SEM micrographs (**Figure 4b**). These

Figure 4. Fracture surface micrographs of (a) GFRP composite laminates without CNTs show clean fiber surface and extensive interfacial debonding at the fiber-matrix interface suggesting weak adhesion between matrix and fiber. (b) 0.75 phr CNTs/GFRP composite laminates exhibit a dimpled/scalloped fracture feature. These composites do not display a direct matrix debonding from the fiber surface

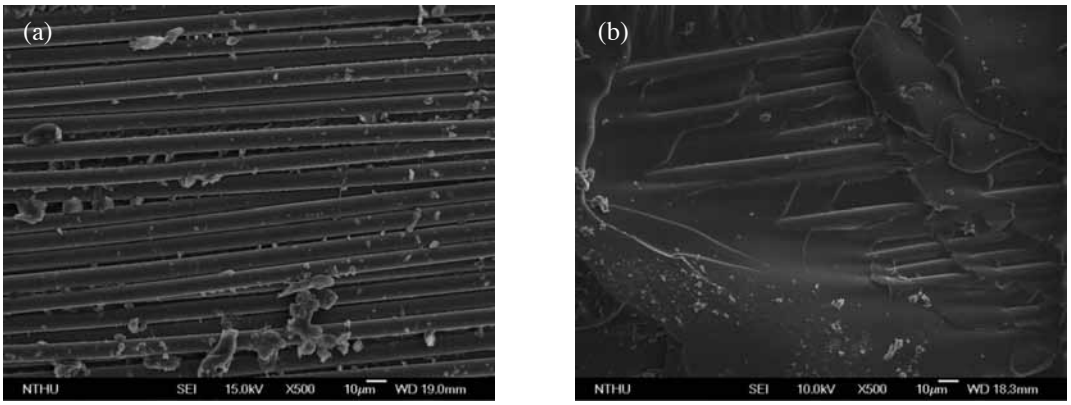

Figure 5. SEM micrograph of (a) an ILSS fracture surface. The CNTs are well dispersed between glass fiber. A region around the glass-fibers shows crack pinning and crack deflection phenomenon. (b) the same specimen at a higher magnification. The network-like structure is formed by the MWCNT

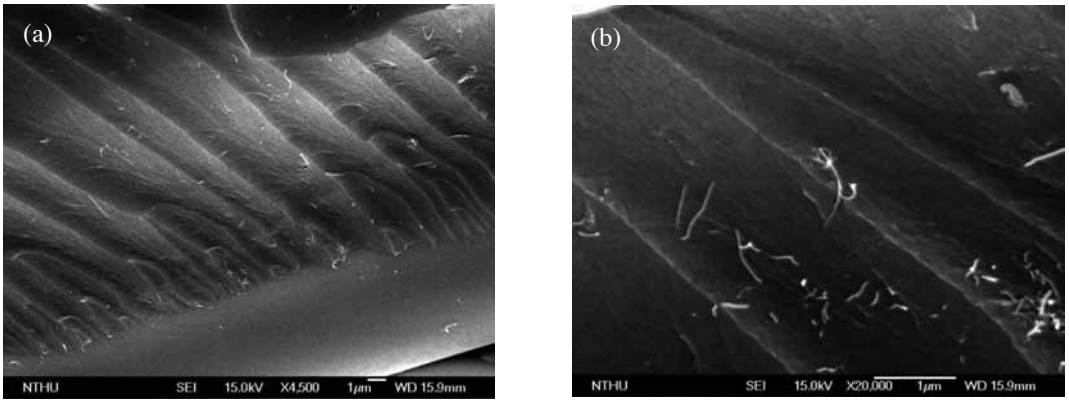

composites do not display direct matrix debonding from the fiber surface. A thin layer of matrix can be seen completely covering the fiber surface indicating resin adhesion. In fact, the fracture failure occurs due to resin cracking and deformation mostly within the matrix near the fiber surface.

The fracture morphologies of CNTs/GFRP composite laminates show (**Figure 5a**) that there are CNTs at the fracture surface of the white line and it exhibits a dimpled/scalloped fracture feature. The crack pinning and crack deflection happened on the fracture surface, while in most areas the CNTs were still firmly in the matrix (**Figures 5a** and **5b**). This phenomenon reveals the great influence of CNTs surface groups on the interfacial bounding. Only if CNTs firmly adhere to the epoxy matrix does the load transfer from the epoxy resin to the CNTs. From the images, it can be observed that the MWCNTs were well-dispersed in the matrix without any aggregations.

3.2 Flexural Tests

Experimental values for the flexural test of CNTs/GFRP composite laminates are given in **Figure 6**. The flexural strength of the GFRP composite laminates is about 250 MPa, while that of the system with 0.75 phr infusion is 272 MPa, a 9.2% flexural strength enhancement. The strength begins to degrade with 1 phr loading. The dispersion of CNTs that restricts the mobility of polymer chains under loading improved the strength in small loadings. The high aspect ratio, high modulus, strength of CNTs and a good interfacial adhesion between the CNTs and matrix also contributed to the reinforcement. However, the decrease of strength with high CNT

content can be attributed to the non-uniform dispersion of CNTs in higher loading system.

3.3 Dynamic Mechanical Analysis

The dynamic properties *versus* temperature for a specimen from the GFRP and GFRP with MWCNT (0.75 phr) composite laminates are shown (**Figures 7a** and **7b** respectively). The DMA plots of the tan delta *versus* temperature for composite laminates are also shown. T_g, determined from the peak position of tan delta, decreased unremarkably from 118.06 °C to 117.38 °C.

The storage moduli for the GFRP and GFRP with MWCNT (0.75 phr) composite laminates are shown in **Figure 8**, and the respective T_g peaks are indicated by arrows. Changes in the storage modulus reflect changes in the polymer matrix and/or the fiber-matrix interface, because the glass fiber modulus does not change in the temperature range studied. Note that for engineering purposes, the useful operating range of a thermoset epoxy is considered to be the range over which the storage moduli is nearly constant[17]. The composite laminate's useful operating range extends to approximately 95 °C. It appears that up to 100 °C, within the glass transition region, the storage modulus of the CNTs/GFRP composite laminates increases as compared to the GFRP composite laminates. This is because the well-dispersed CNTs could form a network, which bears load and improves the storage modulus. The viscoelastic characteristics of the GFRP and CNTs/GFRP composite laminates have a significant effect on the temperature dependence of strength, as shown in the following section.

3.4 Strength and Modulus of the Composite Laminates at High Temperature

The ILSS, flexural strength and bending modulus were measured at test

Figure 6. Effect of CNT contents on flexural strength of GFRP composite laminates

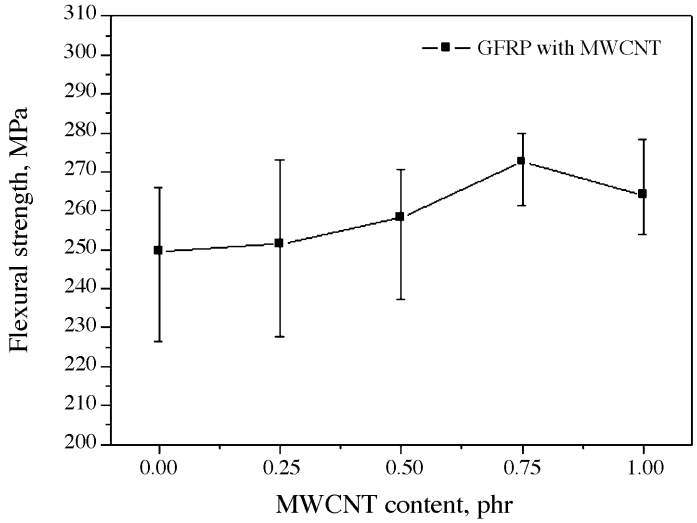

Figure 7. DMA data for (a) GFRP composite laminates (b) 0.75 phr CNTs/GFRP composite laminates

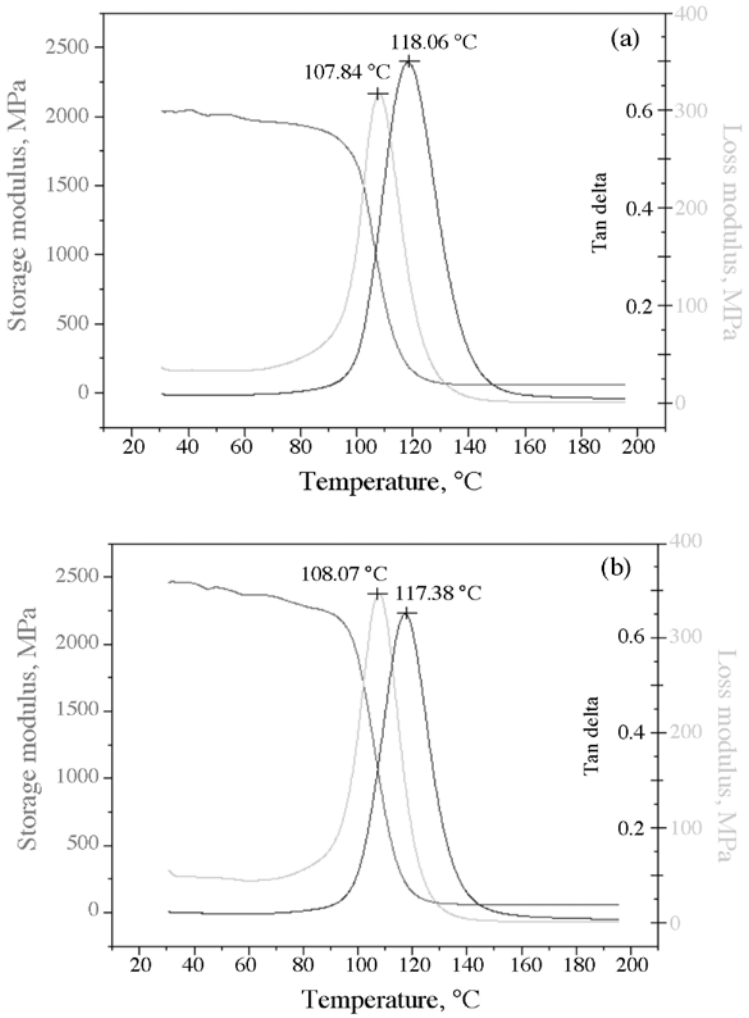

Figure 8. Storage modulus curves for GFRP and 0.75 phr CNTs/GFRP composite laminates

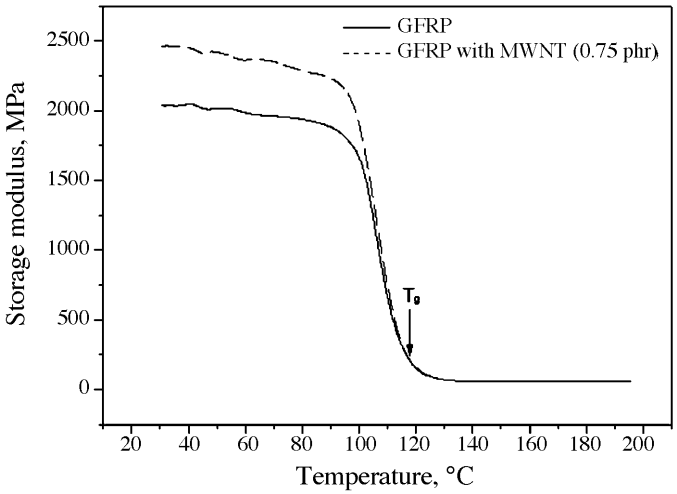

temperatures up to 200 °C to gage the temperature-dependence of the GFRP and GFRP with MWCNTs (0.75 phr) composite laminates. **Figures 9a**, **9b**, and **9c** show ILSS, flexural strength and bending modulus *versus* test temperature for the two prototypes, respectively. As 0.75 phr CNTs are added to GFRP composite laminates it can be found that the tendencies of the ILSS curve, the flexural strength curve, and bending modulus curve, are shifted to the top compared to the GFRP composite laminates. Because adding CNTs improves the ability of stress transfer between matrix and fibers, and restricts the mobility of polymer chains under loading, the strength and modulus were improved. The observed high-temperature strength and modulus

Figure 9. (a) ILSS curves for GFRP and 0.75 phr CNTs/GFRP composite laminates; (b) Flexural strength curves for GFRP and 0.75 phr CNTs/GFRP composite laminates; (c) Bending modulus curves for GFRP and 0.75 phr CNTs/GFRP composite laminates

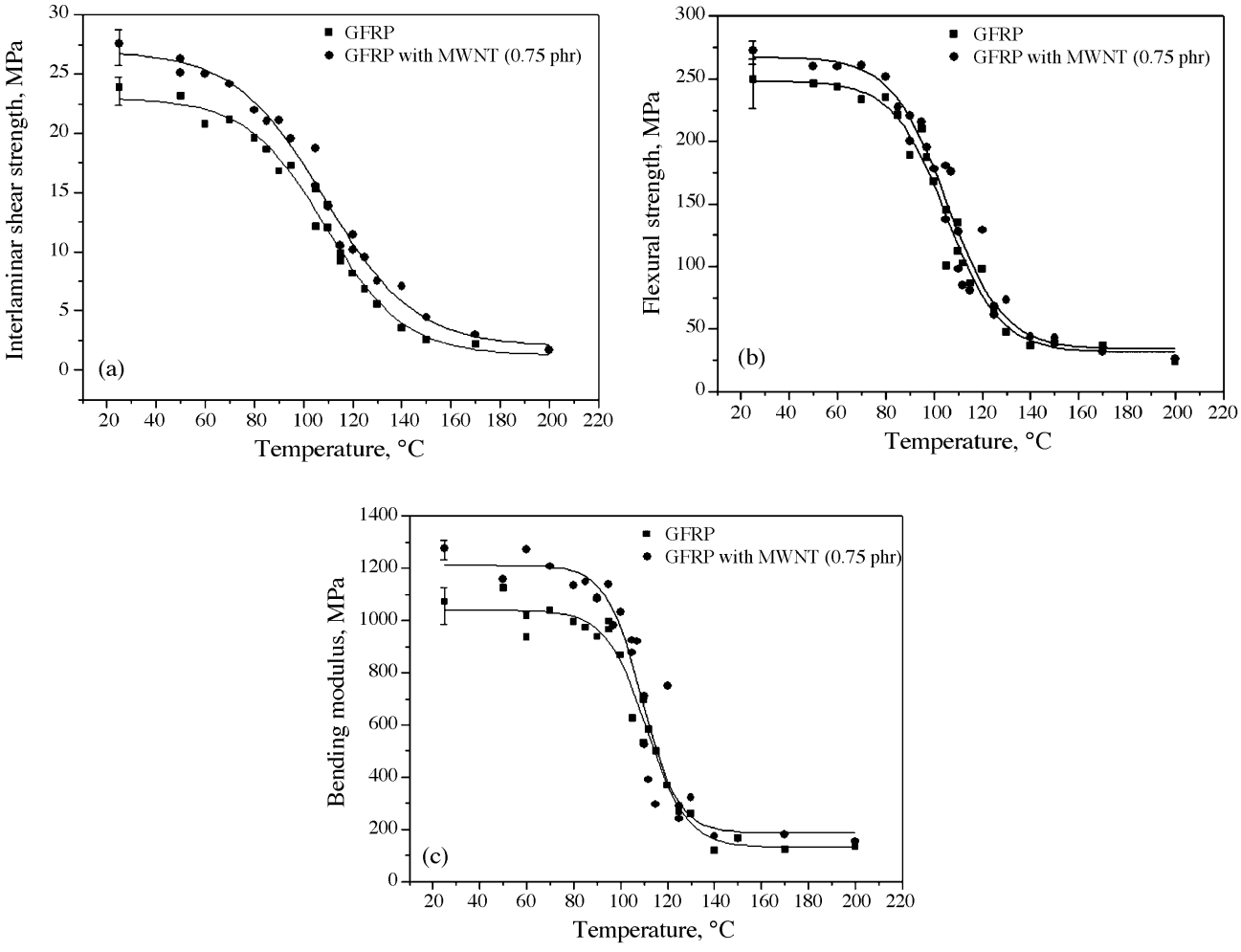

degeneration can be attributed to the matrix softening and the coefficients of thermal expansion (CTE) mismatch between glass-fiber and matrix. Because of the differential CTE between glass fiber and matrix, further residual stress developed at the glass fiber-matrix interface. The residual stress may weaken the glass fiber-matrix interface and/or the thermoset epoxy resin of the composite laminates, promoting the interlaminar failure (crack) across this interfacial region as shown in **Figure 10**.

Figures 11a and **12a** show the images of polished cross-sections of the GFRP and CNTs/GFRP composite laminates of the ILSS fracture at 130 °C (above T_g). It can be observed that the failure modes of GFRP and CNTs/GFRP composite laminates were interlaminar failure. The matrix had lost much of its ability to transfer the stress between glass fibers at this temperature. Moreover, it presents an apparent loss of bonding between glass fiber and matrix as shown in **Figure 11b** and **12b**. High-temperature environment results in reduced mechanical properties due to loss of fiber-matrix adhesion and matrix softening. The fiber-matrix adhesion is most likely to control the overall mechanical behavior of GFRP composite laminates. It was found that ILSS was significantly enhanced by CNTs of high-temperature properties up to 200 °C. The dominate failure mechanism in the ILSS test was fiber-matrix interface failure and matrix cracking. Adding CNTs can improve the ability to transfer the stress between the matrix and fibers. However, no significant influence was found of the flexural strength and bending modulus of high-temperature, because the flexural strength and bending modulus of a composite material mainly depend on the fiber, not on the matrix and fiber-matrix interface.

Figure 10. Small fiber-matrix debondings are present in the GFRP composite laminate ILSS test at 130 °C, because differential CTE between glass fiber and matrix caused further residual stress at the glass fiber-matrix interface

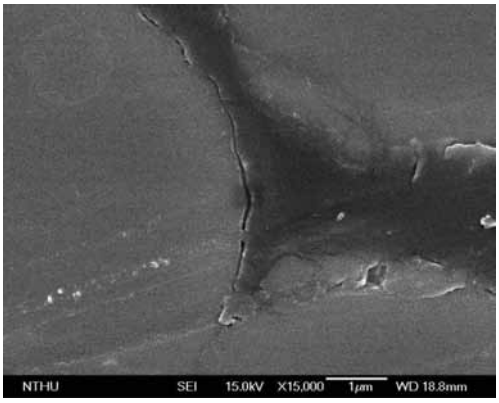

Figure 11. SEM micrograph shows (a) a specimen of GFRP composite laminate ILSS test at 130 °C. When subjected to shear loading, GFRP composite laminate faced delamination between the fiber layers at many places. (b) 10 μm scale bar magnification

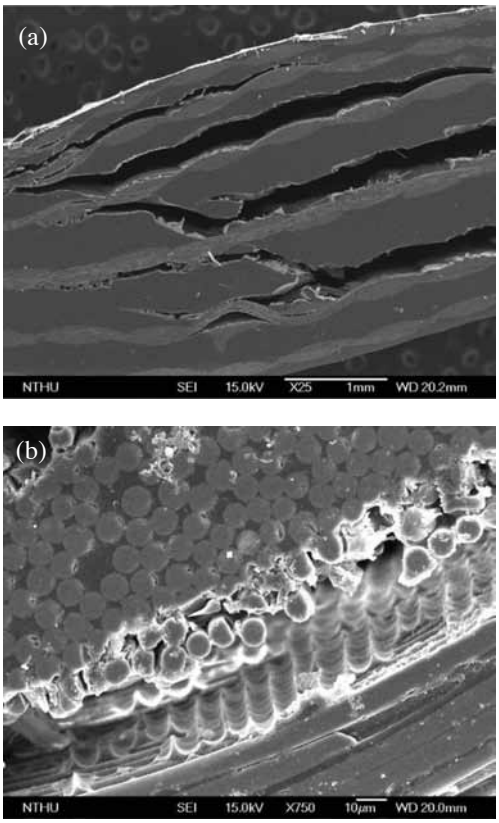

3.5 Interlaminar Shear Strength, Flexural Strength, Bending Modulus and Storage Modulus

The behavior of the storage modulus for the GFRP and CNTs/GFRP composite laminates shows temperature dependent trends similar to those observed for ILSS, flexural strength and bending modulus. **Figures 13a** and **13b** show the normalized ILSS, flexural strength and bending modulus superimposed with the normalized storage modulus for the respective composites. These figures demonstrate a striking correlation between the temperature dependence of the storage modulus and the ILSS, flexural strength

Figure 12. SEM micrograph shows (a) a specimen of the 0.75 phr CNTs/GFRP composite laminate ILSS test at 130 °C, when subjected to shear loading, GFRP composite laminate faced delamination between the fiber layers at many places. The network-like structure formed by the MWCNTs can be recognized as small bright spots between the fiber woven. (b) 10 μm scale bar magnification

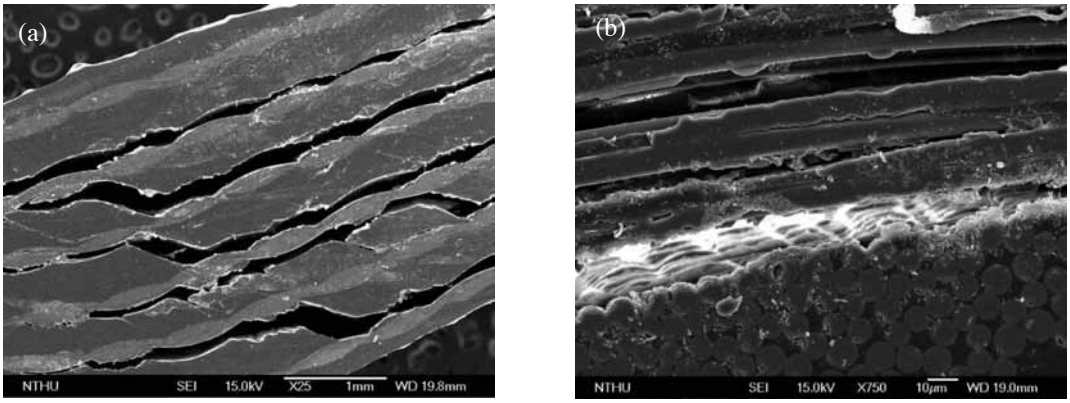

Figure 13. (a) Normalized ILSS, flexural strength, bending modulus and storage modulus for GFRP composite laminate. (b) Normalized ILSS, flexural strength, bending modulus and storage modulus for 0.75 phr CNTs/GFRP composite laminate

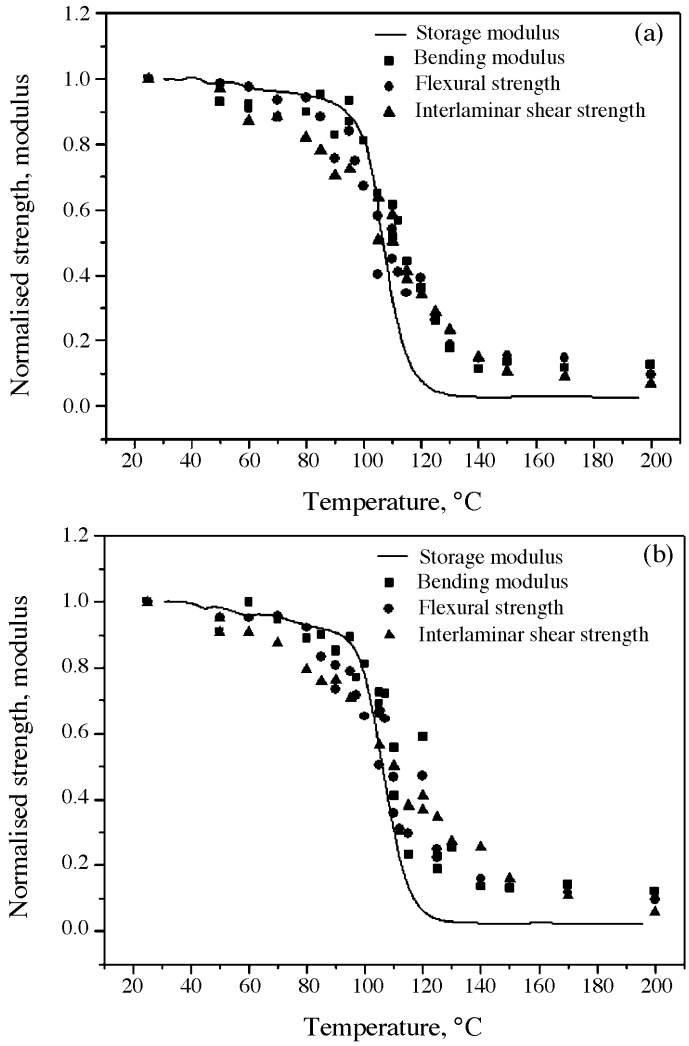

and bending modulus for the prototype composites. The storage modulus thus provides a useful indicator of the temperature dependence of the ILSS, flexural strength and bending modulus of these composites. The correlation between the temperature dependence of storage modulus, ILSS, flexural strength and bending modulus can be understood in terms of shear stresses at the fiber-matrix interface. ILSS, flexural strength, bending modulus and storage modulus were measured by ILSS test, flexural test and DMA, respectively. These tests all use the three-points bending mode. Bending loads are applied perpendicular to the glass fibers, and the measured properties are sensitive to changes in the matrix and/or the fiber-matrix interface. That was a major factor affecting the strength and modulus reduction observed at high temperature. We assert that there is a striking correlation between ILSS, flexural strength, bending modulus and storage modulus for the GFRP and CNTs/GFRP composite laminates.

4. CONCLUSIONS

The mechanical properties of CNTs/GFRP composite laminates were improved significantly with the addition of CNTs. The most significant improvements of ILSS (15.7%) and

flexural strength (9.2%) were at 0.75 phr CNTs content. The crack pinning and crack deflection happened exactly on the fracture surface, while in most areas the CNTs were still firmly in the matrix. This phenomenon reveals the great influence of CNTs surface groups on the interfacial bounding. Only if CNTs firmly adhere to the epoxy matrix does the load transfer from the epoxy resin to the CNTs.

The ILSS, flexural strength and bending modulus were significantly enhanced by CNTs at different temperatures. It appears that up to 100 °C, within the glass transition region, the storage modulus of the CNTs/GFRP composite laminates increases as compared to that of the GFRP composite laminates, because the well dispersed CNTs could form a network, which bears load and improves the storage modulus. A correlation was observed between the temperature dependences of the storage modulus, ILSS, flexural strength and bending modulus in GFRP and CNTs/GFRP composite laminates. The measured properties are sensitive to changes in the matrix and/or the fiber-matrix interface. That was a major factor affecting the strength and modulus reduction observed at high temperature.

REFERENCES

1. Baker A.A., Callus P.J., Georgiadis S., Falzon P.J., Dutton S.E., and Leong K.H., An affordable methodology for replacing metallic aircraft panels with advanced composites, *Composites: Part A*, **33** (2002) 687-696.
2. Wichmann M.H.G., Sumfleth J., Gojny F.H., Quaresimin M., Fiedler B., and Schulte K., Glass-fibre-reinforced composites with enhanced mechanical and electrical properties – Benefits and limitations of a nanoparticle modified matrix, *Engineering Fracture Mechanics*, **73** (2006) 2346-2359.
3. Iijma S., Helical microtubules of graphitic carbon, *Nature*, **354** (1991) 56-58.
4. Song Y. and Youn J., Influence of dispersion states of carbon nanotubes on physical properties of epoxy nanocomposites, *Carbon*, **43** (2005) 1378-1385.
5. Florian H.G., Malte H.G., Bodo F., Wolfgang B., and Karl S., Influence of nano-modification on the mechanical and electrical properties of conventional fibre-reinforced composites, *Composites: Part A*, **36** (2005) 1525-1535.
6. Kim S.G., Chu W.S., Jung W.K., and Ahn S.H., Evaluation of mechanical and electrical properties of nanocomposite parts fabricated by nanocomposite deposition system (NCDS), *Journal of Materials Processing Technology*, **187-188** (2007) 331-334.
7. Zhou Y., Pervin F., Lewis L., and Jeelani S., Fabrication and characterization of carbon/epoxy composites mixed with multi-walled carbon nanotubes, *Materials Science and Engineering A*, **475** (2008) 157-165.
8. Calvert P., Nanotube composites: a recipe for strength, *Nature*, **399** (1999) 210-211.
9. Thostenson E.T., Li C. and Chou T.W., Nanocomposites in context, *Composites Science and Technology*, **65** (2005) 491-516.
10. Gojny F.H., Wichmann M.H.G., Fiedler B., and Schulte K., Influence of different carbon nanotubes on the mechanical properties of epoxy matrix composites - A comparative study, *Composites Science and Technology*, **65** (2005) 2300-2313.
11. Veedu P.V., Anyuan C., Xuesong L., Kougen M., Caterina S., Swastik K., Pulickel M., and Mehrdad N., Multifunctional composites using reinforced laminae with carbon-nanotube forests, *Nature Materials*, **5** (2006) 457-462.
12. Allaoui A., Bai S., Cheng H.M. and Bai J.B., Mechanical and Electrical Properties of a MWNT/Epoxy Composite, *Composites Science and Technology*, **62** (2002) 1993-1998.
13. Tai N.H., Yeh M.K. and Liu J.H., Enhancement of the Mechanical Properties of Carbon Nanotube/ Phenolic Composites using a Carbon Nanotube Network as the Reinforcement, *Carbon*, **42** (2004) 2774-2777.
14. Vincenzo L. and Yao N., Molecular mechanics of binding in carbon-nanotube-polymer composites, *Journal of Materials Research*, **15** (2000) 2770-2779.
15. Thostenson E.T. and Chou T.W., Aligned multi-walled carbon nanotube-reinforced composites: processing and mechanical characterization. *Journal of Physics D: Applied Physics*, **35** (2002) 77-80.
16. Lau K.T., Interfacial Bonding Characteristics of Nanotube/ polymer Composites, *Chemical Physical Letter*, **370** (2003) 399-405.
17. Menard K.P., Dynamic mechanical analysis: a practical introduction to techniques and applications, New York: CRC Press, Boca Raton, 1999.